

Multiple Diffusion–Freezing Mechanisms in Molecular Hydrogen Films

T. Makiuchi,* K. Yamashita, M. Tagai, Y. Nago, and K. Shirahama†

Department of Physics, Keio University, Yokohama 223-8522, Japan

(Dated: August 20, 2019)

Molecular hydrogen is a fascinating candidate for quantum fluid showing bosonic and fermionic superfluidity. We have studied diffusion dynamics of thin films of H₂, HD and D₂ adsorbed on a glass substrate by measurements of elasticity. The elasticity shows multiple anomalies well below bulk triple point. They are attributed to three different diffusion mechanisms of admolecules and their “freezing” into localized state: classical thermal diffusion of vacancies, quantum tunneling of vacancies, and diffusion of molecules in the uppermost surface. The surface diffusion is active down to 1 K, below which the molecules become localized. This suggests that the surface layer of hydrogen films is on the verge of quantum phase transition to superfluid state.

Light molecules such as hydrogen[1, 2] and helium form quantum fluids and solids, in which quantum effects emerge. If hydrogen molecules are kept delocalized at low temperatures, exchange between molecules bring about quantum effects. Among the quantum effects, superfluidity in liquid phase (and even in solid, so called supersolidity) is an extraordinary but a fundamental phenomenon caused by macroscopic quantum coherence. Although study of superfluid helium has spanned almost a century, novel superfluids such as ultracold atoms[3], and condensates of polaritons[4] and magnons[5, 6] have innovated research fields of condensed matter physics. Molecular hydrogen can be unique superfluids[7, 8]: Two nuclear spin isomers in bosonic H₂ and D₂, namely ortho and para states, produce spin-dependent Bose–Einstein condensates. HD, the fermionic isotope, is even more interesting as it may produce anisotropic superfluids in which Cooper pairs possess unprecedented internal degrees of freedom.

In contrast to helium, bulk liquid hydrogen (e.g. H₂) solidifies below 13.8 K and shows no superfluidity because of stronger attraction than that of helium. Efforts of realizing superfluidity in H₂ have therefore been concentrated to weaken the intermolecular attractive forces by reducing dimension or system size [9–11]. The only indication of superfluidity was found in an experiment of nanoclusters with about fifteen H₂ molecules[12]: They cannot be regarded as a macroscopic quantum effect. Experiments to search for superfluidity in H₂ films on solid surfaces and H₂ in confined geometries were unsuccessful[13, 14], and simulations are controversial on the existence of superfluid phase[9, 15].

In this work, we have studied the dynamics of thin hydrogen films by a new technique of elasticity measurement. The elastic study is motivated by our recent finding in helium and neon films[16, 17]. ⁴He films show superfluidity when the coverage n exceeds a critical value n_c ($\sim 20 \mu\text{mol}/\text{m}^2$, roughly 1.8 layers)[16]. The emergence of superfluidity occur as a quantum phase transition (QPT) between localized solid and superfluid at $n = n_c$. We have found that ⁴He, ³He, and ²⁰Ne films show an “elastic anomaly”, in which the elastic constant

of localized films measured with AC strain increases at low temperatures with an excess dissipation. In ⁴He and ³He films, the characteristic temperature of the stiffening decreases as n approaches n_c . The elastic anomaly is quantitatively explained by thermal activation of helium atoms from the localized states to mobile, extended states with energy gap Δ . The gap Δ decreases to zero obeying a power law $\Delta \propto (n - n_c)^\alpha$ with $\alpha \sim 1.3$ (1.8) for ⁴He (³He). Therefore, the critical coverage n_c is identified as a coverage at which the elastic anomaly disappears by gap closure, and (super)fluidity emerges as helium atoms occupy the extended states. On the other hand, in neon film, similar elastic anomaly is observed but the characteristic temperature does not decrease below 5 K: The energy gap does not close and neon film does not show QPT.

These results suggest that elastic anomaly can examine the existence of QPT and superfluidity in adsorbed molecules. In this Letter, we apply this idea to films of three hydrogen isotopes, H₂, D₂, and HD. We have found multiple elastic anomalies in hydrogen films, unlike the single elastic anomaly in helium and neon films. Each elastic anomaly corresponds to a “freezing” of diffusive motion of hydrogen molecules. They are identified as classical thermal diffusion, quantum tunneling, and surface diffusion. Although no QPT was observed, the uppermost surface layer of hydrogen films is on the verge of QPT to superfluid state.

The elastic measurement was carried out with the same torsional oscillator (TO) used in the previous helium and neon studies[16, 17]. The TO consists of a cylindrical BeCu torsion rod embedded with a porous glass rod and a metal bob [see Fig. 1(a)]. The porous glass called Gelsil has three-dimensionally connected nanopores [see Fig. 1(b)]. From a N₂ adsorption isotherm, we obtained the surface area $S = 166 \text{ m}^2$, the total pore volume $v_p = 0.184 \text{ cm}^3$, the peak value of the pore diameter $d_p = 3.9 \text{ nm}$, and the porosity $p = 0.54$. If we consider the nanopore a cylindrical pore with uniform diameter, the mean diameter is $\bar{d} = 4.4 \text{ nm}$, which is about 11 times larger than the diameter of a hydrogen molecule. The TO was mounted on a plate thermally linked to the mixing

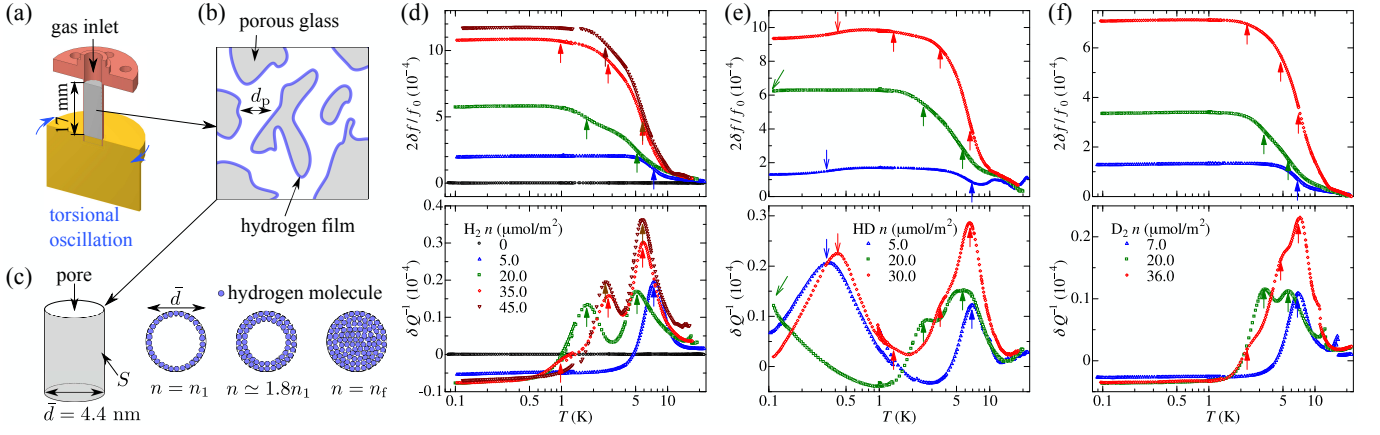


FIG. 1. (a) Cross-section of the torsional oscillator. (b) Schematic cross-section of the porous glass. (c) Cylindrical representation of the pore, and sketches of the monolayer, two-layer and full-pore coverages. (d–f) Temperature dependence of the normalized resonant frequency shift and the excess dissipation of (d) H_2 , (e) HD, and (f) D_2 . The upward arrows indicate peaks of δQ^{-1} and locally maximal slopes in $2\delta f/f_0$. The data of $2\delta f/f_0$ in (e) and (f) are vertically shifted to set $2\delta f/f_0 = 0$ at high T . Only in HD data (e), a dissipation peak accompanied with decrease in $2\delta f/f_0$ is indicated by downward arrows (see text).

chamber of a dilution refrigerator.

The coverage n is the amount of dosed molecules divided by S . The coverage at which a monolayer is formed [see Fig. 1(c)] is estimated to be $n_1 = (v_m^2 N_A)^{-1/3}$, where N_A is the Avogadro constant and v_m the molar volume. Using $v_m = 23.30, 21.84,$ and $20.58 \text{ cm}^3/\text{mol}$ [18], we get $n_1 = 14.5, 15.2,$ and $15.8 \text{ } \mu\text{mol}/\text{m}^2$ for $\text{H}_2, \text{HD},$ and D_2 , respectively. The amount of molecules at which the pore is fully filled (the full-pore) is $n_f = v_p/Sv_m$, and we have $n_f = 47.6, 50.8,$ and $53.9 \text{ } \mu\text{mol}/\text{m}^2$ for $\text{H}_2, \text{HD},$ and D_2 , respectively. To avoid solidification, hydrogen gas [19] was introduced through a capillary which was thermally isolated from cold stages. The film was then annealed above the triple point temperature T_{tp} (13.8, 16.6, and 18.7 K for $\text{H}_2, \text{HD},$ and D_2 , respectively) followed by slow cooling down to 0.1 K. The data was taken during a warming from 0.1 to 1.3 K with normal operation of dilution refrigerator, and a subsequent warming from 1.0 to 22 K without circulating ^3He . Data at 1.0–1.3 K were doubly measured due to this procedure. No critical effect was observed from the annealing conditions and possible ortho–para conversion.

The resonant frequency f and energy dissipation Q^{-1} of torsional oscillation represents the elastic constant and energy loss of the substrate-hydrogen composite system. We refer to the frequency and dissipation without hydrogen film ($n = 0$), $f_B(T)$ and $Q_B^{-1}(T)$, as the background. When the hydrogen film is formed on the pore surface, f and Q^{-1} change by the elastic contribution of the film. The elastic constant and dissipation of the hydrogen film are given by a normalized frequency shift $2\delta f/f_0$ and an

excess dissipation δQ^{-1} , where

$$\delta f(T) = f(T) - f_B(T), \quad (1)$$

$$\delta Q^{-1}(T) = Q^{-1}(T) - Q_B^{-1}(T). \quad (2)$$

Figure 1(d) shows $2\delta f/f_0$ and δQ^{-1} of H_2 film as a function of T . At a small coverage of $n = 5.0 \text{ } \mu\text{mol}/\text{m}^2$ ($\sim 0.3n_1$), $2\delta f/f_0$ increases toward low T with a single peak of δQ^{-1} at $T_p = 7.5 \text{ K}$. $2\delta f/f_0$ has the largest slope at the dissipation peak temperature T_p . The negative value of δQ^{-1} at low T indicates that the hydrogen film reduces the internal loss of the porous glass. These behaviors of the elastic anomaly are qualitatively similar to those observed in the helium and neon films [16, 17]. However, at coverages of 20.0, 35.0, and 45.0 $\mu\text{mol}/\text{m}^2$, δQ^{-1} has multiple peaks, unlike in the helium and neon cases. The number of peaks are two at 20.0 and 45.0 $\mu\text{mol}/\text{m}^2$, and three at 35.0 $\mu\text{mol}/\text{m}^2$. At $n = 45.0 \text{ } \mu\text{mol}/\text{m}^2$ ($\sim n_f$), the pore is almost filled with H_2 . For every coverage, the high- T value of $2\delta f/f_0$ almost equals the background value, meaning that the hydrogen film is soft (even below T_{tp}), while the low- T value of $2\delta f/f_0$ has a T -independent increment, which means that the film is stiff. The shear modulus given by a formula [17] $G = (G_{g0}/0.197)(2\delta f/f_0)/(1-p)^2$ is 190 MPa at 45.0 $\mu\text{mol}/\text{m}^2$ at low- T . This is the same order of magnitude as $G = 100 \text{ MPa}$ of solid hydrogen [1].

The multiple elastic anomalies were also observed in HD and D_2 films. This is shown in Fig. 1(e) and 1(f). In the HD and D_2 experiments, $2\delta f/f_0$ sometimes showed unexpected shifts in the entire T range after changing n . We attribute these T -independent shifts to an effect of vibrational disturbance. We set $2\delta f/f_0 = 0$ at high T by vertically shifting the data. In HD films, we observed fourth dissipation peak accompanied with a slight

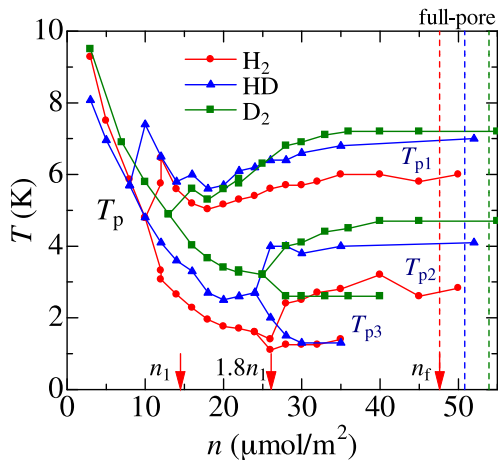


FIG. 2. The coverage dependence of the dissipation peak temperature T_p . The monolayer (n_1), the two-layer ($1.8n_1$), and the full-pore (n_f) coverages of H_2 are indicated by arrows.

decrease of $2\delta f/f_0$ below about 1 K, i.e., the HD film is slightly softened at lowest temperatures. This anomaly was seen only in HD, and the origin is unknown. We will not discuss this fourth anomaly in this Letter.

In the previous helium and neon studies [16, 17], it was established that the elastic anomaly originates from anelastic relaxation process with thermal activation of molecules [20, 21]. The relation between the activation energy (the energy gap), E , and the thermal relaxation time, τ , is $\tau = \tau_0 \exp(E/k_B T)$, where τ_0^{-1} is the attempt frequency. When $\omega\tau \gg 1$ (low T) with $\omega = 2\pi f$, the molecules are localized, thus $\delta f > 0$. On the other hand, when $\omega\tau \ll 1$ (high T), the molecules are frequently activated to mobile states during deformation of the substrate, therefore δf is essentially zero. The crossover occurs at T_p at which δQ^{-1} has a peak and $\omega\tau(T_p) = 1$.

The multiple dissipation peaks indicate that the hydrogen film freezes by different mechanisms that have unique activation energies. The coverage dependencies of T_p 's are displayed in Fig. 2. The overall features of T_p are similar among H_2 , HD, and D_2 . The curve of T_p splits twice into branches. We label the peak temperatures at the branches in descending order, i.e., $T_{p1} > T_{p2} > T_{p3}$, as indicated in Fig. 2. The curve of T_{p1} appears at a coverage less than n_1 , and the curve of T_2 appears at the two-layer coverage $n_2 \simeq 1.8n_1$. The curves of T_{p1} and T_{p2} persist until $n > n_f$, but the dissipation peak corresponding to the curve of T_{p3} disappears at about 40 $\mu\text{mol}/\text{m}^2$. This is shown as the termination of the T_{p3} curve. From these behaviors, we conclude that T_{p1} and T_{p2} are related to activation energies in solid hydrogen, and T_{p3} originates from activation in the surface of films. It is remarkable that these diffusion mechanisms are indistinguishable below about 10 and 25 $\mu\text{mol}/\text{m}^2$ where two branches of T_p merge.

T_{p1} shows a shallow minimum at about 18 $\mu\text{mol}/\text{m}^2$

and stays constant (5–7 K) at higher coverages. The coverage dependence of T_{p1} is *quantitatively* similar to that of T_p of neon film [17]. This is explained by the fact that the Lennard–Jones potentials for hydrogen and neon are almost identical [22]. Therefore, the first anomaly around T_{p1} is caused by classical molecular interaction.

The ratio $T_{p1}/T_{p2} \sim 2$ is common to all isotopes. In bulk solid hydrogen, two self-diffusion mechanisms are expected [23]. One is the classical thermal diffusion of vacancies in solid, and the other is the quantum tunneling of vacancies. The classical diffusion is related to T_{p1} . The activation energies for the thermal diffusion and the quantum tunneling are $E_v + E_b$ and E_v , respectively, where E_v is the vacancy formation energy and E_b is the potential barrier. As the ratio holds $(E_v + E_b)/E_v \sim 2$ for solid H_2 and D_2 [23], we conclude that T_{p2} of our system is related to the quantum tunneling.

T_{p3} vanishes as n approaches n_f . This is due to the disappearance of the surface of the film as the film thickens inside nanopores [see Fig. 1(c)]. Therefore, the third anomaly T_{p3} is attributed to the diffusion in the surface of the film. It has been suggested that the surface layer of hydrogen films is mobile at low temperatures [24–26]. The surface diffusion at low temperatures is because the motion of molecules at the uppermost layer does not require formation of vacancy [25]. The elastic anomaly at T_{p3} clearly indicate the existence of the surface fluid state in all the isotope films down to 1–2 K, a temperature of one tenth of the triple point.

We extract the activation energy by fitting the multiple elastic anomalies to the following model function. Every single elastic anomaly is described by the dynamic response function [16],

$$z_i = \left(\frac{\delta G}{G_0} \right)_i \left[1 - \int_0^\infty \frac{F_i(E)}{1 - i\omega\tau_0 \exp(E/k_B T)} dE \right], \quad (3)$$

where $(\delta G/G_0)_i$ is the relaxed shear modulus divided by the shear modulus of the torsion rod, $F_i(E)$ gives the distribution of the activation energy, and i denotes the index of the elastic anomaly. The normalized frequency shift and excess dissipation are the real and imaginary part of z_i , respectively. We assume $F_i(E) = (1/\sqrt{2\pi}\sigma_i E) \exp(-[\ln(E/\Delta_i)]^2/2\sigma_i^2)$ (the lognormal distribution) as the best choice [16, 17], where Δ_i is the median of the activation energy and σ a dimensionless parameter. For the multiple elastic anomalies, the total dynamic response function is

$$Z = \sum_{i=1}^N z_i, \quad (4)$$

where $N = 1, 2$, or 3 is the number of the anomaly. A result of fitting, $2\delta f/f_0 = \text{Re}(Z)$ and $\delta Q^{-1} = \text{Im}(Z)$ with $N = 3$, is shown in Fig. 3. The model reproduces the step-by-step increase of $2\delta f/f_0$ and multiple peaks of

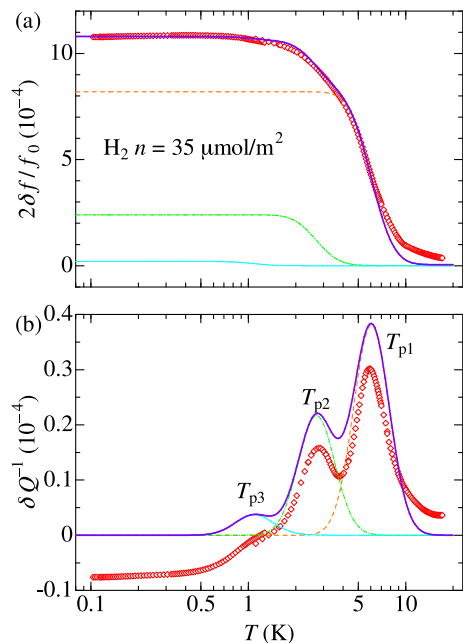


FIG. 3. A fitting result for (a) $2\delta f/f_0$ and (b) δQ^{-1} with three peaks. The orange, green and blue curves are the fittings for each dissipation peaks using Eq. (3). The purple curve is the sum represented by Eq. (4).

TABLE I. The dissipation peak temperatures and the activation energies at the highest coverages in units of K.

	T_{p1}	T_{p2}	T_{p3}	Δ_1/k_B	Δ_2/k_B	Δ_3/k_B
H ₂	6.0	2.8	1.1	340	72	13
HD	7.0	4.1	1.3	420	180	15
D ₂	7.2	4.7	2.6	420	260	30

δQ^{-1} . The dissipation from the model agrees with the experimental result, except that δQ^{-1} of the experiment has some additional T -dependent background as in the neon case [17].

The ratio of $2\delta f(T \ll T_p)/f_0$ to $\delta Q^{-1}(T_p)$ is essential for determining τ_{0i} . If the ratio is 0.5, $F_i(E)$ is the delta function (no distribution) and $\tau_{0i} = \omega^{-1} \exp(k_B T_{pi}/\Delta_i)$. If the ratio is smaller than 0.5, as in the present results, τ_{0i} may be smaller in the order of magnitude. We obtained $\tau_{01}, \tau_{02} \sim 10^{-12}-10^{-30}$ s for T_{p1} and T_{p2} , which are very small similarly to the neon case, and $\tau_{03} = 1 \times 10^{-9}$ s which is almost equal to the value in the helium case. The parameter σ_i was always about 0.3. The activation energy Δ_i was strongly dependent on T_{pi} . The fitting parameters at the highest coverages (n_f for T_{p1} and T_{p2} , and $\sim 40 \mu\text{mol}/\text{m}^2$ for T_{p3}) are shown in Table I.

We discuss the values of the activation energies. The activation energies of the classical diffusion in bulk solids were calculated to be $(E_v + E_b)/k_B = 197$ K (H₂) and 290 K (D₂) [23]. Our results of Δ_1/k_B 's give higher val-

ues. The activation energies for the quantum tunneling in bulk, i.e., energy to create vacancies, were $E_v/k_B = 112$ K (H₂) and 132 K (D₂) [23]. Our results of Δ_2/k_B are larger in D₂ but smaller in H₂. The larger values of Δ_i are attributed to the molecular confinement in nanopores. The activation energies in the first and second layers on the substrate can be larger than that of bulk because these layers are strongly bound and compressed. In the case of H₂, the larger zero-point fluctuation may reduce Δ_2 .

For the surface diffusion, Δ_3 's roughly agree with activation energies in previous studies; $E_s/k_B = (19 \pm 2)$ (H₂) [25], (43 ± 7) K (H₂) [26], (16.1 ± 0.5) K (HD) [24], and (38 ± 4) K (D₂) [25]. The differences in quantity are probably due to the differences of the film thickness and the substrate. Our results of Δ_i give relatively small values.

T_{p3} 's in Fig. 2 do not decrease below 1 K. This means that hydrogen films do not undergo a QPT, contrary to helium [16]. However, the concave curvatures of T_{p3} of hydrogen and T_p of helium are very similar in $n_1 < n < 1.8n_1$. Moreover, the ratio $\Delta_3/k_B T_{p3}$ is 12 for H₂, HD, and D₂ films. It agrees well with $\Delta/k_B T_p = 13$ of ⁴He and ³He films [17]. These similarities between hydrogen and helium strongly suggest that the third elastic anomaly in hydrogen films is also originated from a quantum many-body ground state, such as Mott insulator or Mott glass [27]. Δ_3 is regarded as a Mott gap, and at finite temperatures the surface molecules are excited to spatially extended states. The surface layers are *on the verge of a QPT to (super)fluid state*.

Finally, we propose that, if the surface molecules are excited at low temperatures by artificial means, e.g. emission of phonons with frequency $\omega > \Delta_3/\hbar$, they can be macroscopically condensed and exhibit superfluidity in a non-equilibrium sense. Study of the relaxation rate from excited to ground states is needed to examine the feasibility of non-equilibrium superfluidity.

To conclude, we discovered multiple elastic anomalies in all hydrogen isotope films, in which the elastic constant has multiple steps accompanied with dissipation peaks. The multiple anomalies correspond to the ‘‘freezing’’ of different diffusion mechanisms: the classical thermal diffusion, the quantum tunneling, and the surface diffusion of molecules. The uppermost surface of the films is in a quantum many-body ground state, which is on the verge of a quantum phase transition to (super)fluid state. Our finding in this work implies new approaches to the realization of superfluidity in hydrogen films.

This work has been supported by JSPS KAKENHI Grant No. JP17H02925, JP17K18762, and JP19K21856. T.M. was supported by Grant-in-Aid for JSPS Research Fellow JP18J13209.

-
- * Current address: Department of Applied Physics, The University of Tokyo, Bunkyo 113-8656, Japan.
[†] keiia@phys.keio.ac.jp
- [1] I. F. Silvera, *Rev. Mod. Phys.* **52**, 393 (1980).
[2] J. Van Kranendonk, *Solid Hydrogen: Theory of the Properties of Solid H₂, HD and D₂* (Springer, New York, 1983).
[3] M. H. Anderson, J. R. Ensher, M. R. Matthews, C. E. Wieman, and E. A. Cornell, *Science* **269**, 198 (1995).
[4] J. Kasprzak, M. Richard, S. Kundermann, A. Baas, P. Jeambrun, J. M. J. Keeling, F. M. Marchetti, M. H. Szymańska, R. André, J. L. Staehli, V. Savona, P. B. Littlewood, B. Deveaud, and L. S. Dang, *Nature* **443**, 409 (2006).
[5] A. S. Borovik-Romanov, Y. M. Bunkov, V. V. Dmitriev, and Y. M. Mukharskiy, *JETP Lett.* **40**, 1033 (1984).
[6] S. O. Demokritov, V. E. Demidov, O. Dzyapko, G. A. Melkov, A. A. Serga, B. Hillebrands, and A. N. Slavin, *Nature* **443**, 430 (2006).
[7] V. L. Ginzburg and A. A. Sobyenin, *Sov. Phys. JETP Lett.* **15**, 242 (1972).
[8] H. J. Maris, G. M. Seidel, and T. E. Huber, *J. Low Temp. Phys.* **51**, 471 (1983).
[9] M. C. Gordillo and D. M. Ceperley, *Physical Review Letters* **79**, 3010 (1997).
[10] S. A. Khairallah, M. B. Sevryuk, D. M. Ceperley, and J. P. Toennies, *Phys. Rev. Lett.* **98**, 183401 (2007).
[11] F. Mezzacapo and M. Boninsegni, *Physical Review Letters* **100**, 145301 (2008).
[12] S. Grebenev, B. Sartakov, J. P. Toennies, and A. F. Vilesov, *Science* **289**, 1532 (2000).
[13] O. E. Vilches, *J. Low Temp. Phys.* **89**, 267 (1992).
[14] R. H. Torii, H. J. Maris, and G. M. Seidel, *Phys. Rev. B* **41**, 7167 (1990).
[15] M. Dusseault and M. Boninsegni, *Phys. Rev. B* **97**, 205403 (2018).
[16] T. Makiuchi, M. Tagai, Y. Nago, D. Takahashi, and K. Shirahama, *Phys. Rev. B* **98**, 235104 (2018).
[17] T. Makiuchi, K. Yamashita, M. Tagai, Y. Nago, and K. Shirahama, *J. Phys. Soc. Jpn.* **88**, 034601 (2019).
[18] H. M. Roder, G. E. Childs, R. D. McCarty, and P. E. Angerhofer, *Survey of the Properties of the Hydrogen Isotopes Below Their Critical Temperatures*, Technical Note 641 (National Bureau of Standards (U.S.), 1973).
[19] The sample gas purity reported by the supplier was 99.99999%, 97%, and 96% for H₂, HD, and D₂, respectively.
[20] A. S. Nowick and B. S. Berry, *Anelastic Relaxation in Crystalline Solids* (Academic Press, New York and London, 1972).
[21] R. H. Tait and J. D. Reppy, *Phys. Rev. B* **20**, 997 (1979).
[22] L. H. Nosanow, *J. Low Temp. Phys.* **26**, 613 (1977).
[23] C. Ebner and C. C. Sung, *Phys. Rev. A* **5**, 2625 (1972).
[24] M. Maruyama, M. Bienfait, F. C. Liu, O. E. Vilches, and F. Rieutord, *Surf. Sci.* **283**, 333 (1993).
[25] K. G. Sukhatme, J. E. Rutledge, and P. Taborek, *J. Low Temp. Phys.* **103**, 301 (1996).
[26] E. Bloss and A. F. G. Wyatt, *J. Low Temp. Phys.* **119**, 743 (2000).
[27] T. Giamarchi, P. L. Doussal, and E. Orignac, *Phys. Rev. B* **64**, 245119 (2001).